



Basic Characteristics and Evolution of Geological Structures in the Eastern Margin of the Qinghai-Tibet Plateau

Dejie Deng¹, Changliu Wang^{2*}, Peihao Peng³

¹College of Earth Sciences, Chengdu University of Technology, Chengdu, 610059, China

²Architecture and Urban Planning College, Southwest Minzu University, Chengdu, 610041, China

³College of Tourism and Urban-Rural Planning, Chengdu University of Technology, Chengdu, 610059, China

* Corresponding author: clwang19@163.com

ABSTRACT

Based on field geological survey and stratigraphic profile survey in the eastern margin of the Qinghai-Tibet Plateau, the basic characteristics and evolution of geological structure in the eastern margin of the Qinghai-Tibet Plateau are studied. The Dongyuan area of the Qinghai-Tibet Plateau is divided into the late Cenozoic period and the current period. During the Late Cenozoic, the Pliocene Xigeda lacustrine deposits develops from 4.2 MaBP to 2.6 MaBP, with 9 cold-warm climate change stages. There are 4.3 MaBP old glacial period in this area, and 5 extreme paleoclimate events in Quaternary. At present, the horizontal movement intensity and mode of different tectonic zones are determined by the northward extrusion, eastward extrusion and rotation around the eastern tectonic junction in the study area, and the stages of the movement state changing with time are related to the gestation and occurrence of extra-large earthquakes. At present, the three-dimensional crustal movement shows that the tectonic activity differentiation of mountain and basin, which is related to tectonic dynamic environment and deep material activity, is related to the compression, shortening and uplift of plateau mountain and the extension and subsidence of basin, reflecting the inheritance of neotectonic activity. Through practical analysis, it is found that the eastern margin of the Qinghai-Tibet Plateau is composed of Minshan fault block and Longmenshan structural belt. The left-lateral dislocation of Minjiang fault is roughly the same as the vertical dislocation. In Longmenshan tectonic belt, the right-lateral dislocation of Maowen-Wenchuan fault, Beichuan-Yingxiu fault and other main faults is the same as the vertical dislocation.

Keywords: Qinghai-Tibet Plateau; Eastern margin area; Geological structure; Basic characteristics; Evolution research; Crustal movement.

Características básicas y evolución de las estructuras geológicas en el margen oriental de la meseta Qinghai-Tibet

RESUMEN

En este trabajo se estudian las características básicas y la evolución de la estructura geológica en el margen oriental de la meseta Qinghai-Tibet con base en el análisis geológico de campo y el estudio del perfil estratigráfico de la zona de estudio. El área de Dongyuan de la meseta Qinghai-Tibet se divide en el período Cenozoico tardío y el período actual. Durante el Cenozoico Tardío, los depósitos lacustres del Plioceno Xigeda se desarrollaron de 4.2 MaBP a 2.6 MaBP, con 9 etapas de cambio climático frío-cálido. Hay 4.3 MaBP viejos períodos glaciales en esta área, y cinco eventos paleoclimáticos extremos en el Cuaternario. En la actualidad, la intensidad del movimiento horizontal y el modo de las diferentes zonas tectónicas están determinados por la extrusión hacia el norte, la extrusión hacia el este y la rotación alrededor de la unión tectónica oriental en el área de estudio, y las etapas del cambio del estado del movimiento con el tiempo están relacionadas con la gestación y ocurrencia de terremotos extragrandes. En la actualidad, el movimiento cortical tridimensional muestra que la diferenciación de la actividad tectónica de la montaña y la cuenca, que está relacionada con el entorno dinámico tectónico y la actividad del material profundo, está relacionada con la compresión, el acortamiento y la elevación de la meseta de montaña y la extensión y hundimiento de cuenca, que refleja la herencia de la actividad neotectónica. A través del análisis práctico, se descubre que el margen oriental de la meseta Qinghai-Tibet está compuesto por el bloque de falla Minshan y el cinturón estructural Longmenshan. La dislocación lateral izquierda de la falla de Minjiang es aproximadamente la misma que la dislocación vertical. En el cinturón tectónico de Longmenshan, la dislocación lateral derecha de la falla de Maowen-Wenchuan, la falla de Beichuan-Yingxiu y otras fallas principales es la misma que la dislocación vertical.

Palabras clave: meseta Qinghai-Tibet; Área del margen oriental; Estructura geológica; Características básicas; Investigación de la evolución; Movimiento de la corteza.

Record

Manuscript received: 27/04/2019

Accepted for publication: 25/09/2019

How to cite item

Deng, D., Wang, C., & Peng, P. (2019). Basic Characteristics and Evolution of Geological Structures in the Eastern Margin of the Qinghai-Tibet Plateau *Earth Sciences Research Journal*, 23(4), 283-291. DOI: <https://doi.org/10.15446/esrj.v23n4.84000>

Introduction

The eastern margin of the Qinghai-Tibet Plateau mainly refers to the region between the eastern Himalayan tectonic knot and the western Qinling orogenic belt. The Eastern Kunlun fault system borders the western Qinling Mountains in the north, the Longmenshan tectonic belt borders the Yangtze block in the east, and the Sichuan-Yunnan block in the southwest, i.e. the southeastern margin of the Qinghai-Tibet Plateau (including Eastern Tibet, Western Sichuan, Yunnan, Central and Eastern Myanmar, China-Myanmar-Lao-Vietnam border region, but mainly Sichuan-Yunnan region) bounded by the SN-oriented all-right-lateral strike-slip fault system and the Yushu-Xianshuihe-Xiaojiang arc fault system (Wang, Tang, & Wang, 2017). Geotectonically, the area is the convergence zone of Yangtze block, Songpan-Ganzi block, Lanping-Simao block, Baoshan block, Lushui-Longling block, Gangdise-Tengchong block and other micro-blocks. During Cenozoic, the area underwent multi-stage magmatic activities and strong tectonic deformation, which resulted in many fault structure with different scales and properties (Liang et al. 2017). During the neotectonic period, especially during the Quaternary or Late Quaternary, under the dynamic background of the continuous collision between the Indian plate and the Eurasian plate, the crustal movement in this area is very active. There are many active faults with different scales, types and activities, which are also the most prominent strong earthquake active zones in China. Activities are characterized by high frequency and intensity, and are accompanied by Quaternary volcanic activities, such as the famous Tengchong volcanic area (Jiang, Ruan, & Chen, 2016).

The process of Neotectonic deformation and its dynamic mechanism in the eastern margin of the Qinghai-Tibet Plateau, the present pattern of active tectonic deformation, and the relationship with large earthquakes are all issues of great concern in the field of geological science at home and abroad (Yang, Miao, Dan, Liu, & Wang, 2017). Because these problems are closely related to the present crustal deformation mode and its dynamic mechanism of the Qinghai-Tibet Plateau and even the whole East Asian continent, and to the uplift process of the Qinghai-Tibet Plateau and its genetic mechanism, the correct understanding of the neotectonic movement law and the characteristics of active tectonic system on the eastern margin of the Qinghai-Tibet Plateau is also the correct establishment of Kinematic model for crustal deformation process and the key to exploring its dynamic mechanism in the present Qinghai-Tibet Plateau (Feng, Gao, Yang, Hui, & Zhou, 2017). Therefore, this area has been the key area to deeply understand the current crustal deformation mode and its dynamic mechanism in the Qinghai-Tibet Plateau and East Asia, and to explore the eastward extrusion of material in the plateau and its regulation mode (Zhang et al., 2016). Around the above problems, predecessors have done a lot of work in neotectonics and active structures, seismogeology, geophysics and so on, and have put forward many models or viewpoints on the latest structural deformation mode and its dynamic mechanism in this area. Among them, the most representative ones are the outlaw-shaped tectonic system, the extrusion or rotation mode of Sichuan-Yunnan rhombic block, the continental escape mode, the rotation movement mode of fault block and the lower crustal flow mode. The above viewpoints have important influence on the deep understanding of neotectonic movement and active tectonic deformation mode in this area. However, with the emergence of new data, especially new achievements in active fault research, geophysical exploration and GPS observation, it is difficult to fully explain the current mode of crustal activity, dynamic mechanism and its relationship with strong earthquake activity and migration in this area due to the limitation of technical means and research level at that time (Wei, Guo, Yao, Zhu, & Wang, 2016). Therefore, by studying the basic characteristics and evolution of geological structures in the eastern margin of the Qinghai-Tibet Plateau, we can systematically obtain the latest crustal deformation process, the temporal and spatial framework of Neotectonic evolution and other important continental dynamic background information, reconstruct the active tectonic system and kinematic geological model of the area, and consolidate the seismogenic area of the area. The basis of geological work is not only helpful to further understand the latest crustal deformation process and mechanism of the Qinghai-Tibet Plateau, to scientifically evaluate the future trend of large earthquakes in the region, but also to provide a more reliable geological basis for the rational planning, development and utilization of regional territory and the evaluation of crustal stability of major engineering projects (Hu et al., 2016).

Materials and Methods

Late Cenozoic Tectonics

Age and Environment of Pliocene Xigeda Lake Facies Deposition on the Eastern Margin of the Qinghai-Tibet Plateau

A set of fluvial and lacustrine deposits were widely developed in the Dadu River and Anning River basins during the Pliocene, indicating that there was a lake development period in the eastern margin of the Qinghai-Tibet Plateau, which was the Pliocene Pan-lake Period. This study is of great significance in discussing the coupling relationship between Pliocene paleoenvironmental changes and uplift of the plateau. Haiziping section in Luding and Zhoujiagou section in Mianning are typical sections of Xigeda River lacustrine deposits in the western Sichuan Plateau (Yi & Wang, 2016). The lake facies stratigraphic section of Haiziping Lake in Luding begins in Ganhaizi and ends at Wantou and Dengzhangwo through Jindongzi. The total thickness is 440.5m, which is divided into 15 layers. The Zhoujiadagou section in Mianning is located in Zhoujiadagou, Fengcao Village, about 7 km north of the county town. The total thickness of the section is 300.7m. It can be roughly divided into two sections according to lithology, namely, the yellow layer with 103.5m thickness and the grey layer with 197.2m thickness. It can be divided into 18 layers.

Previous scholars have studied the Xigeda Formation in Western Sichuan. There have been different opinions on the sedimentary age of the Xigeda Formation, which directly affects the study of the Paleoenvironment of the fluvial and lacustrine facies strata. In this paper, high resolution magnetic stratigraphic samples of typical sections in this area with spacing of 25 cm to 50 cm are sampled and tested on the superconducting magnetometer of Institute of Geomechanics and Institute of Geology and Geophysics, Chinese Academy of Sciences. The results of magnetic strata and environmental records obtained by superconducting magnetometer show that the Haiziping section is mainly formed in the Gauss period, with the development ages ranging from 4.2 MaBP to 2.6 MaBP. The geological age belongs to the middle and late Pliocene. The Xigeda Formation in Luding is the earliest section in the Xigeda lacustrine facies. The Zhoujiagou section of the Anning River Basin is also formed in the Gauss Period. The boundary between Gauss positive polarity and Gilbert negative polarity is 297.2m in the Mianning Xigeda Formation, and the sedimentation time is about 3.58Ma-2.6Ma. According to the above results, the preliminary results of magnetic stratigraphy of Xigeda Formation distributed in Dadu River, Anning River and Jinsha River valley are very consistent and can be well compared. The Xigeda Formation is mainly formed during the Gauss positive polarity period, probably beginning at about 4.2 Ma and ending at 2.6 Ma at the earliest (Xiao, Tan, Hu, Zhou, & He, 2017).

The results of magnetostratigraphy provide a chronological guarantee for the study of long-time-scale paleoenvironmental changes recorded in Xigeda lacustrine deposits. Environmental indicators such as organic matter content, grain size and sporopollen in the time frame provide information on Pliocene environmental changes in the eastern margin of the plateau. The environmental records of organic carbon content in Haiziping profile show that the lowest value of organic carbon is 0.14%, the highest value is 1.04%, and the average value is 0.38%. Organic carbon records show that the palaeoenvironmental changes in Haiziping area of Luding have undergone nine stages of palaeoclimate change: cool→ warm →cold →warm →cold→ cold →cold →cool. Six warm→ cool cycles have appeared in the Xigeda deposit of Mianning. Pollen and isotope analysis also recorded the periodic variation of paleoclimate during the period of 4.2 MaBP to 2.6 MaBP (Chen et al., 2016). Based on the preliminary study of the evolution pattern of paleoenvironment during Pliocene in Western Sichuan, a new understanding of the relationship between paleoenvironment changes in the eastern margin of the Qinghai-Tibet Plateau and the stage uplift of the whole plateau has been obtained.

Geological Characteristics of Quaternary Glaciers on the Eastern Margin of the Qinghai-Tibet Plateau

The eastern margin of the Qinghai-Tibet Plateau is a part of the eastern extension of the plateau, with an average altitude of over 3500 m. The East-West mountain ranges on the plateau have turned into nearly north-south mountain ranges in this area, which is a transitional area from the first step

to the second step of Chinese geomorphology. Late Cenozoic glacial deposits are well developed in the eastern part of the Qinghai-Tibet Plateau, which is a typical area for the development of Quaternary paleoglaciers in the transitional zone between the eastern and western parts of the mainland of China. Many scholars have studied the Quaternary glaciers in this area and discussed the glacial evolution and global change of the Qinghai-Tibet Plateau, which has a good working basis. Several paleoglaciers have been discovered in recent years. The discovered glacial remains have been chronologically studied. The regional Quaternary glacial sequence has been established and the regional paleoclimate and paleoenvironment changes in the Late Cenozoic have been discussed (Jie, Ya, De, & Gao, 2017).

A set of 43 m gravel beds is developed at the lacustrine bottom of Xigeda Formation in Luding, western Sichuan, with the geographic coordinates of 29°54'50.4" in the North latitude, 102°12'51.0" in the East longitude, and elevation of 1940 m. According to the analysis of gravel sedimentary characteristics and surface morphology of quartz sand by scanning electron microscopy, it is considered that it belongs to a set of ancient moraine beds. The results of magnetostratigraphic study show that the moraine is formed in the Kirchaty positive polarity event of the Gilbert polar epoch, about 4.3 Ma from now on, which is the oldest Cenozoic glacial age ever discovered in East Asia. At about 10 km in Qionghai, Xichang, a 15 m gravel layer is developed on the eastern side of the Luoji River. Its geographic coordinates are N27°42'42" in the north latitude and 102°21'33" in the East longitude. Its elevation is 2575 m. It is distributed in the watershed of Zemu River and Ezhang River. The gravel layer is a set of purple-grey mud-gravel layer overlying the Daqing Liangzi lacustrine sedimentary stratum. The gravel in the gravel layer mainly comes from Luoji Mountain in the west. The gravel is poorly sorted and has no directional arrangement. The sedimentary characteristics of gravel layer and the results of SEM analysis of quartz sand show that this layer is a typical moraine layer. The Daqing Liangzi moraine layer corrodes with the overlying Daqing Liangzi lake facies deposits. Based on the detailed study of the magnetic strata of the river and lake facies layers, the paleomagnetic calculation shows that the age of the bottom boundary of the Daqing Liangzi Formation is about 2.14 Ma. Therefore, the Daqing Liangzi moraine is deposited in the early Pleistocene, and its absolute age should be earlier than 2.14 million years ago.

A set of gravel layers is developed in the back hill of Jiancao Village, 7 km from the north of Mianning County. The geographic coordinates are 28 33.738' in the north latitude and 102 12.610' in the East longitude, and the altitude is 1972 m. The gravel layers extend southward to the canteen where 108 National Highway meets the Anning River. The thickness of gravel layer in Jiancao is about 20m. It is a mixed accumulation of gray-white and gray-yellow clay, silt and gravel. The gravel weathers strongly, and its separation and grinding are poor. There are fractured glaciers and streaks which have not been completely disconnected. There are many groups of scratches on the gravel. The bottom of the gravel layer is grey-black claystone and siltstone of Xigeda Formation in Gauss period, which are unconformity contact relations. The discovery of sedimentary fabrics, fractured rocks and streaked rocks and the occurrence of distant granite drift gravel indicate that the maple channel gravel layer should be a typical moraine layer (Wang, Tang, & Wang, 2017). At the same time, the results of scanning electron microscopy of quartz sand particles in gravel layer show that the gravel layer has the characteristics of shell fracture, parallel cleavage and parallel scratch, which further proves that the gravel layer is glacial origin. In the study of the age of the moraine gravel layer in Jiancao, ESR dating samples are collected from the upper, middle and lower parts of the gravel layer. The ages of the upper, middle and lower samples are 822,000 years, 1012,000 years and 128,800 years, respectively. They are deposited in the middle and late Pleistocene, roughly in the same period as the thick loess L9-L15 in the Loess Plateau.

The Quaternary glacier development sequence in the eastern part of the Qinghai-Tibet Plateau can be established based on the determination of cosmic nuclide age of moraines in Tanggula Mountain, the north-central section of Shaluli Mountain and the Zheduo Mountain and the study of ²¹Ne, ¹⁰Be and ²⁶Al ages of glacial debris. The results of radionuclide dating show that there are three glacial stages in Tanggula Mountains, and one glacial stage develops before 180kaBP. The smaller glacial advance occurs before 68kaBP. The oldest glacial moraine in Tanggula Mountains has a high degree of weathering and distributes on the front plateau of Tanggula Mountains. The last glacial period developed in Litang-Yidun Haizishan area. The time window of cosmic

nuclide exposure is 17 kaBP-7 kaBP, and the penultimate glacial period is also developed. There are two glacial stages in Zheduoshan area. The last glacial exposure age is 19 kaBP to 24 kaBP. The older glacial moraines advance to Zheduotang, Kangding. There are three grade overlying loess moraine platforms on the North Bank of Zagunao in the east of Lixian County, western Sichuan Province. The geographic coordinates are 31°26'48.7" in the north latitude and 103°10'10.8" in the East longitude. The ESR age of the gravel layer in the high platform is 691,000 years, that in the middle platform is 613,000 years, and that in the low platform is 79,000 years. The gravel layer in the high platform and the middle platform represents the two stages of large-scale glacial development in this area. In the northern part of the Shaluli Mountains, the ancient ice caps of nearly 2000 km² have been developed in the Haizi Mountains of Ganzi and Baiyu. The geographic coordinates of Haizi Mountains in the core area are 31°13'48.7" in the north latitude and 99°51'12.6". The typical glacial remains such as glacial lakes, glacial troughs and valleys, side till dikes, terminal till dikes, polished surfaces, sheep's back stones and glacial debris have been developed in the area. Preliminary studies show that there are two glacial stages in this area. Six complete arc-shaped end-moraine dykes have been developed in Nalengcaogou valley. The cosmic nuclide exposure age of the glacial debris in the central part is 20,000 years. Many moraine dykes represent different stages of glacial retrogression since the last glacial period. The lateral moraine dike on the West Bank of Amara trough valley is earlier than the last moraine dike in Nalengtao, which is the penultimate glacial period. With further study, this area will become one of the typical Quaternary glacier areas in the eastern margin of the Qinghai-Tibet Plateau. In a word, the moraine layer at the bottom of Xigeda Formation in Haiziping, Luding represents the old glacial period 4Ma ago in the eastern margin of the Qinghai-Tibet Plateau. There are five glacial periods in the Quaternary Period. The oldest one is the moraine outcropped from Daqiangliangzi on the eastern side of Luoji Mountain. It is 2.2 million years ago. The second one is the ancient glacier developed from 1 million to 1.1 million years ago in the source area of Anning River. The second one is the ancient glacier from 600,000 to 700,000 years ago, with large scale. It corresponds to the deep-sea O isotope stage 16-18, represented by the high and middle moraine platforms of Zagunaohe River in Lixian County. Another stage is about 200,000 years ago, which is equivalent to stage 6-8 of deep-sea O isotope, represented by moraines on the southern slope of Tanggula Mountains. The last stage is 20,000 to 70,000 years ago, which corresponds to two to four stages of deep-sea O isotope, represented by moraines in Litang Haizi Mountain, Kangding Zheduoshan Mountain and Baiyu Haizi Mountain in Western Sichuan.

Current Construction

Spatial Difference and Time Stage Characteristics of Horizontal Motion Velocity Field in Region

In view of the fact that no major earthquakes occurred in the eastern border area of the Qinghai-Tibet Plateau between 1999 and 2009 since the establishment of the "Network Project", we can approximately regard the long period of GPS horizontal motion velocity field from 1999 to 2009 before the Wenchuan earthquake as the background trend pattern of horizontal motion in the study area to analyze the spatial zoning differences. The temporal characteristics of horizontal motion changes related to the occurrence of large earthquakes (Bu et al., 2016) are analyzed by using the recent motion state from 2009 to 2017 after the earthquake. The horizontal velocity field of the eastern margin of the Qinghai-Tibet Plateau from 1999 to 2009 is shown in Fig. 1.

movement are mainly reflected in the differences of intensity and mode of movement. (1) The difference of movement intensity between different tectonic parts is mainly manifested in the lower horizontal movement rate of the Qinghai-Tibet Plateau and the South China Block, the Ordos Block and the Alxa Block, while the internal movement rate of the plateau increases significantly, reflecting the difference between the intensive activity of the Qinghai-Tibet Plateau and the activity of the relatively stable blocks around it. For example, the GPS velocity vector in Qaidam-Qilian Mountains in the northeastern margin of the Qinghai-Tibet Plateau has been reduced from 15mm/a to 20mm/a in the interior of the plateau to 5mm/a to 10mm/a in the boundary zone of the plateau, even smaller, and the crust has been shortened obviously. The horizontal velocity of GPS stations near the seismogenic

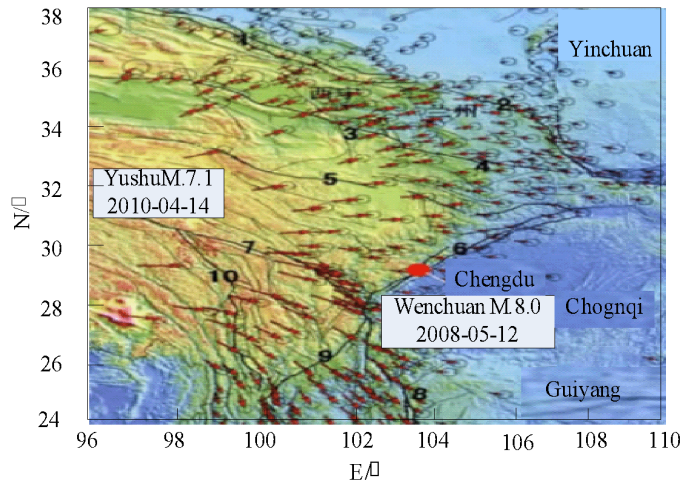


Figure 1. Image of horizontal motion velocity field from 1999 to 2009

structure of the Longmenshan fault zone before the Wenchuan earthquake is smaller, except the horizontal velocity of internal GPS stations in Bayan Hara block is 1/3 or 1/2, especially the relative velocity of the trans-Longmenshan fault zone is less than 1 mm/a. The Wenchuan M8 earthquake in 2008 occurred in the background of the eastern movement of the Bayan Hara massif in the northeastern Qinghai-Tibet Plateau, which was blocked by the South China massif for a long time, and the Honghe fault in southwestern Yunnan Province. The horizontal velocity of clockwise rotation from the southwestern side of the rift to the border between China and Myanmar decreases significantly from north to south. (2) The difference of movement modes is mainly manifested in the clockwise slow torsional movement from NE, NEE and gradually to E-S in the northern part of the eastern margin of the Qinghai-Tibet Plateau. If the Qilian-Haiyuan main fault zone is taken as the boundary, the torsional movement in the southern side is significantly larger than that in the northern side, resulting in significant intense compression and left-lateral shear. In the shape region, the motion is generally characterized by extrusion, thrust and torsion. Besides the eastward movement of the Bayan Hara block hindered by the South China block and characterized by both compression and strike-slip, the central and southern parts of the study area generally exhibit SE-SSE horizontal slip and clockwise rotation around the vertical axis with the Sichuan-Yunnan rhombic block as the main body. The Sichuan-Yunnan rhombic block is NE-oriented in Jianchuan and Lijiang—Xiaojinhe fault is bounded by SE to SSE. In southwestern Sichuan-Yunnan, the NW-oriented Honghe fault is the northern boundary, and its movement rate is obviously weaker than that of Sichuan-Yunnan rhombic block. The direction of movement is gradually shifted from SSE to S. The NW-Yongde Longling and Setang-Mengzha faults near NS in the western margin play a certain role in shielding and absorbing the clockwise movement rate in this area, and the GPS stations in the western side even have the effect of absorbing the clockwise movement rate. The motion in the direction of SSW is presented. These are consistent with the inheritance trend of tectonic movement in the study area since the neotectonic period, reflecting that the present horizontal movement is controlled by the northward compression, eastward extrusion and rotation around the eastern tectonic junction of the Qinghai-Tibet Plateau. The horizontal velocity field images of the eastern margin of the Qinghai-Tibet Plateau from 2009 to 2017 are shown in Fig. 2.

From Figure 2, it can be seen that the overall shape of horizontal movement in the large area during this period seems to be similar to that in the earlier period, but there are still some inconsistencies in some tectonic locations, reflecting that the changes of current horizontal movement in the region have a temporal stage related to large earthquake events. (1) From 2009 to 2017, compared with 1999-2009, the overall movement rate of the Bayan Hara Block towards E-E shifted to S increased, especially in the Wenchuan earthquake area and nearby GPS stations. In addition, the horizontal velocity projection of GPS stations across Longmenshan tectonic belt from the eastern margin of the Bayan Hara massif to the Chengdu plain shows that the SE-SSE horizontal velocity of GPS stations in Wenchuan earthquake-prone zone of

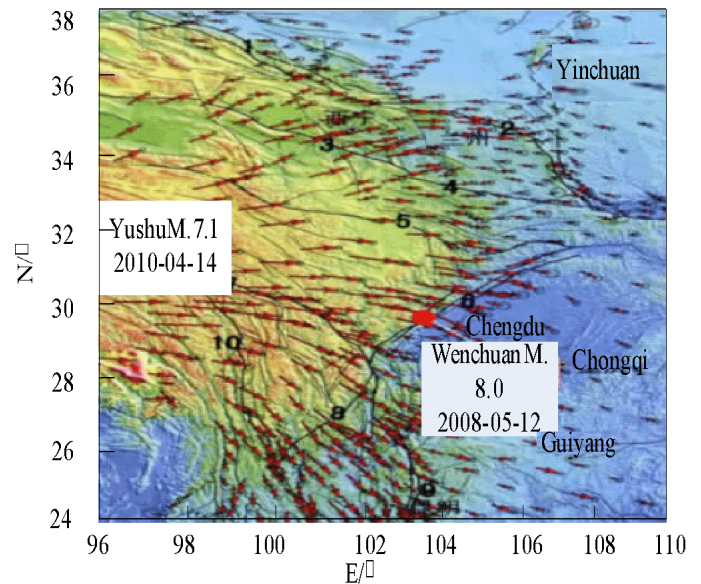


Figure 2. Image of horizontal Motion Velocity Field from 2009 to 2017

Longmenshan fault and its western side is about 20 mm/a from 2009 to 2017, while the velocity of GPS stations in Chengdu plain is still about the same as the previous period. Similarly, the amplitudes of motion on both sides of the fault are quite different (Zhang, Liu, & Huang, 2017). These reflect the dislocation of seismogenic tectonic rupture in Wenchuan Earthquake. The large-scale thrust-dominated crustal extensional movement on the west side of the seismic rupture zone releases the strain energy accumulated by long-term compression and blockade, and is in the state of adjustment relaxation after the earthquake. (2) The movement rate of GPS stations at the southern end of Longmenshan Mountains and the intersection area of Anning River fault, the eastern part of the Sichuan-Yunnan border and the western Qinling tectonic belt to the south of Longmenshan Mountains are relatively reduced, reflecting that these zones are in a state of sustained compression. (3) The clockwise rotational velocity of the Sichuan-Yunnan rhombic block is also increased, and the difference between the strength of the block and that of the outer boundary is more obvious. (4) The SE-oriented motion of GPS stations on the southern side of the Ganzi-Yushu fault, where the seismogenic structure of the Yushu M7.1 earthquake occurred in April 2010, increased, reflecting the influence of left-lateral strike-slip dislocation of the seismogenic structure of the Yushu earthquake on the tectonic activity in this area.

Analysis of 3-D Crustal Movement Characteristics in This Area

In order to analyze and compare the current crustal horizontal and vertical motion reflected by GPS and leveling observations in the eastern margin of the Qinghai-Tibet Plateau, we first use the leveling network in the study area as the starting data, and use the least squares collocation method to calculate the surface fitting, so that the vertical velocity surface data corresponding to the continuous spatial distribution of the region are obtained (Liu, Cai, & Chen, 2017). The vertical motion rate color maps of different regions are drawn with different colors. The rising and falling rate values in the color maps are marked at the bottom of the map with color scale. The red-yellow color represents the area with higher rising rate, and the blue-light blue color represents the area with larger falling rate. Secondly, the horizontal motion velocities of GPS stations in two periods are separately plotted. Vector labeling is used in the color map of regional vertical motion rate, and a more intuitive regional horizontal and vertical three-dimensional crustal motion image is obtained. The image is shown in Figure 3.

By analyzing and comparing the present three-dimensional horizontal and vertical crustal motion images in the eastern margin of the Qinghai-Tibet Plateau shown in Figure 3, it can be seen that the crustal velocity field of regional horizontal motion is relative to the background field of long-

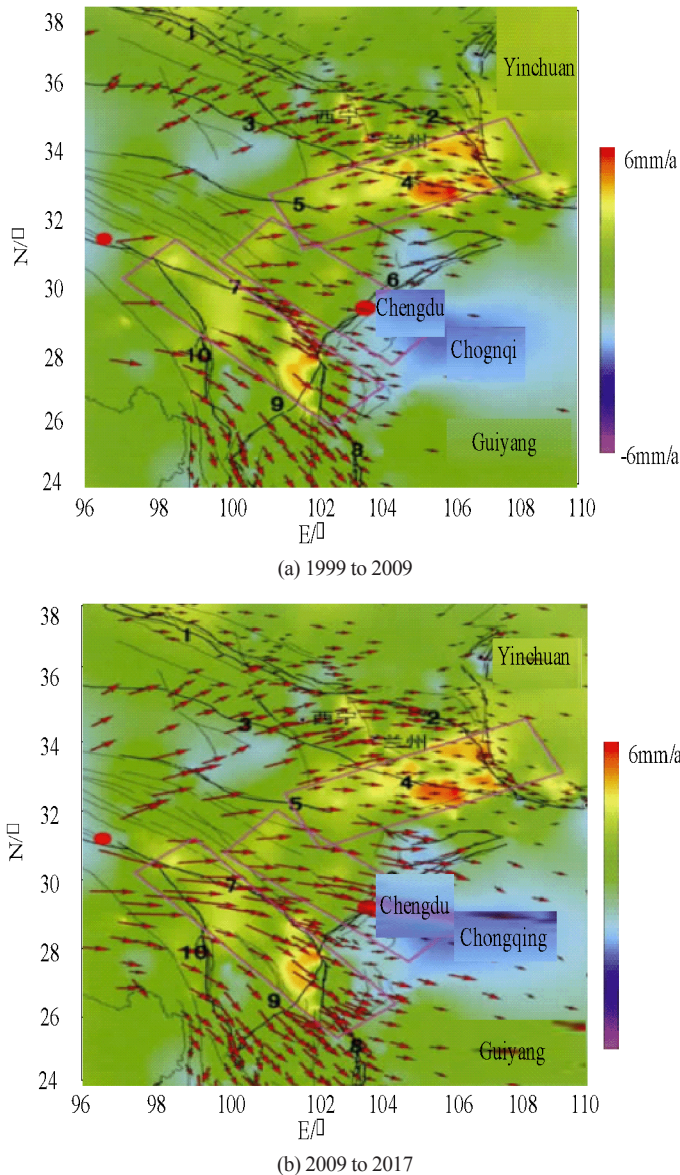


Figure 3. Crustal movement image

time-scale vertical motion, whether in the period of 1999–2009 before the Wenchuan earthquake or in the period of 2009–2017 after the recent earthquake. The vertical uplift movement of the zones with strong horizontal compression-shortening movement is also remarkable, i.e. the red and yellow range in Fig. 3. They have certain symbiotic characteristics, such as the western Qinling Mountains and the vicinity of Liupanshan Mountains in the north of the region, the eastern part of the western Sichuan Plateau in the south of the region, and the northeastern mountain area of the Sichuan-Yunnan rhombic block, etc. Similarly, basins with horizontal extensional movement are mainly subducted vertically, such as Zhongdian-Lijiang area in the south of Sichuan-Yunnan rhombic block and Yinchuan basin in the north of the study area. These reflect that the three-dimensional crustal movement in the eastern margin of the Qinghai-Tibet Plateau under the dynamic environment of extrusion, extrusion and rotation presents the inherited general features and general trend of crustal compression and shortening to form uplift of mountain areas and extensional subsidence of basins. The western Qinling Mountains, Liupanshan Mountains, Qilian Mountains and Helan Mountains in the northern part of the eastern margin of the Qinghai-Tibet Plateau are extruded and uplifted, and the basins are relatively subsided, forming a vertical differential movement gradient zone between the mountains and basins. In the south-central part of the eastern margin of the Qinghai-Tibet Plateau, besides the overall uplift of the western

Sichuan Plateau to the west of the Longmenshan fault, the north-central rise of the Sichuan-Yunnan rhombic block is also significantly different from the South relative subsidence, showing a general trend of east-west extension subsidence and edge compression in the Sichuan-Yunnan block.

On the basis of the above, the zonal areas of strong vertical differential movement and relatively significant horizontal compression movement in the study area are selected, which are SE-oriented across Longmenshan structural belt, NE-oriented across West Qinling fault zone and SSE-oriented across Anning River fault zone on the eastern boundary of Sichuan-Yunnan rhombic block. They are also the seismogenic faults of Wenchuan earthquake and their surrounding structures, shown as the pink rectangular box in Fig. 3. Projection of horizontal motion velocity across fault zone along the direction of dominant velocity of GPS station is obtained. Firstly, from the point of view of the above, the movement state changes of Wenchuan earthquake area and its peripheral related tectonic fault area before and after Wenchuan earthquake are obtained. The horizontal velocity projection of GPS station across Wenchuan seismogenic structure from the eastern margin of the Bayan Hara block to the Chengdu Plain has a dominant direction of SE. From 1999 to 2009 before the Wenchuan Earthquake, the relative horizontal velocity near Longmenshan fault is small and the difference between the two sides of the fault is weak. From 2009 to 2017, the SE-SEE horizontal velocity of GPS stations near Longmenshan fault zone and its west side is about 20 mm/a, while the velocity of GPS stations in Chengdu Plain is still the same as that in the previous period. The great difference in the amplitudes of motion between the two sides of the fissure reflects the dislocation of the seismogenic tectonic rupture of the Wenchuan earthquake. The crustal movement of the western side of the seismic rupture zone, which is dominated by huge thrust, releases the strain energy accumulated by long-term compression and blockade, and is in the post-earthquake adjustment state. Secondly, from the projection maps of horizontal velocity of GPS stations crossing the western Qinling fault zone and the Anning River fault zone crossing the eastern boundary of Sichuan-Yunnan rhombic block in the periphery of the earthquake area, it can be seen that during the long period from 1999 to 2009 before Wenchuan Earthquake, the horizontal velocity of GPS stations on both sides of the fault shows quasi-linear trend distribution; from 2009 to 2017 after Wenchuan Earthquake, the quasi-linear distribution trend of velocity values across faults changes, and the difference of horizontal motion amplitude between the two sides of the fault increases (Li, Zheng, & Peng, 2018). The horizontal motion rate in the south side of the fault in the northern margin of the West Qinling Mountains is obviously higher than that in the north side of the fault, while the horizontal movement in the east and west side of the Anning River fault is stronger and weaker in the East side and the difference is more significant. The former reflects the strong thrust and dextral dislocation of the seismogenic structure of the Wenchuan earthquake, which results in the intensification of compression movement and the possible locking of faults in the western Qinling tectonic belt. The latter may reflect the strong left-lateral dislocation of the Yushu earthquake with M 7.1, triggered by the Wenchuan earthquake, which occurred at the southern boundary of the Bayan-Hara block (Ganzi-Yushu fault). The clockwise rotational acceleration of the Sichuan-Yunnan rhombic block strengthens the compression in the eastern boundary-Anninghe fault zone. Further analysis of the strong vertical uplift and remarkable horizontal compression movement of the two sections shown in Fig. 4 shows that the strain accumulation in the fault zone crossed by the section after the Wenchuan earthquake is still in progress. This is consistent with previous scholars' understanding that Coulomb rupture stress of Wenchuan Earthquake has a role in strengthening stress accumulation in the eastern boundary tectonic areas of the West Qinling and Sichuan-Yunnan Blocks.

Results

Minshan Fault Block

The Minshan fault block originated from the Gonggaling Mountains in the north and passed southward through Hongxingyan, Xuebaoding, Xueguzhai and Maobaoshan, disappearing in the Longmenshan tectonic belt north of Maoxian County. It lies between the near East-West Motianling structural belt

and the north-east Longmenshan structural belt, forming an eastern boundary of the Qinghai-Tibet Plateau. From the deep tectonic background, Minshan fault block is situated in the steep change zone of crustal thickness in the East and west of China, constituting the boundary of two first-order neotectonic units in the strong uplift area in Western China and the weak uplift area in eastern China, and the middle section of the North-South Seismic belt. Minshan fault block is a north-south trending neotectonic uplift, which is quite different from the eastern and Western landforms. Its formation mechanism is closely related to the movement characteristics of the eastern and western boundary faults since the neotectonic period. Huya fault is the eastern boundary of Minshan fault block, which extends in NNW direction, inclines westward with uncertain dip angle. The eastern part of the fault is middle-low mountain area with planation elevation of about 3200 m-3500 m and the western part of the fault is Minshan, with planation elevation of about 4200 m-4500 m. Therefore, the Huya fault should be characterized by a thrusting from west to east, and the planation planes on both sides of the East and West should be broken perpendicularly by about 1000m. Considering the fact that the latest flattened strata in this area are Pliocene laterite slope formation (N2h) and the oldest one after the disintegration of planation plane is early Pleistocene Guanyinshan formation (Wan & Du, 2018), the average vertical slip rate of Huya fault since Quaternary should be about 015 mm/a. The new activity of Huya fault shows clear linear characteristics in aerial and satellite photographs. Along the fault line, fault ridges, fault scarps, fault-fault gullies, alluvial fans and river terraces can be seen. At about 1 km in Xiaohebei, Huya fault cut out of date from the alluvial fan and forms a relatively obvious fault scarp, which results in a left-lateral displacement of the gully forming the alluvial fan of 47 m, as shown in Fig. 4.

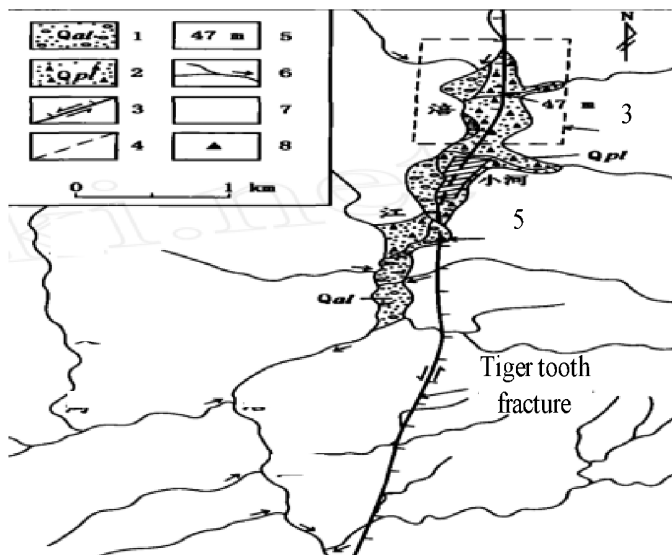


Figure 4. New active trace and fault geomorphology map of Tiger tooth fault near Xiaohu

It can be seen from Fig. 4 that the front of the alluvial fan and the Fujiang's secondary river terrace are in a gradual transition state, and the analysis should belong to synchronous heterogeneous deposits. At the top of the second terrace, the age of sub-sandy soil determined by thermoluminescence method is $32700a \pm 2600a$. Based on this, the average horizontal slip rate of Huya fault since late Quaternary is estimated to be about 114mm/a. Based on this, the average horizontal slip rate of Huya fault since late Quaternary is estimated to be about 114 mm/a. It is interesting to note that the Huya fracture cut a small dry ditch on the alluvial fan at a depth of only 0.3m-0.5m and a width of about 4m-5m with a left-handed dislocation of 413m, as shown in Figure 5.

From Figure 5, it can be seen that the lateral edge walls and pipelines on both sides of Xiaogangou are synchronously left-handed staggered, with good consistency. It is very likely that they are the co-seismic dislocations of the Songpan-Pingwu earthquake of M 7.2 in 1976. Minjiang fault is the western boundary of Minshan fault block, which constitutes the boundary between Songpan-Ganzi orogenic belt and Motianling block. The fault originates from

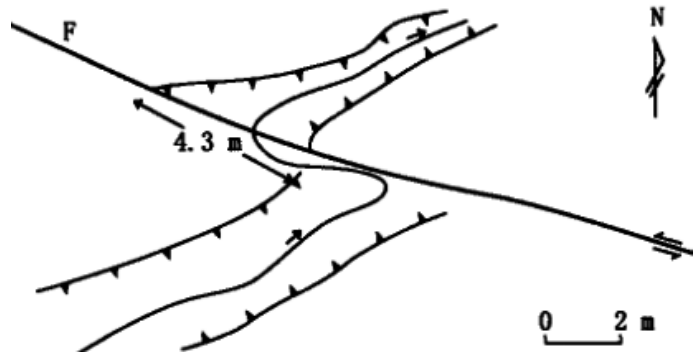


Figure 5. Rupture horizontal dislocation dry ditch

the north of Gonggaling Mountains and is intercepted by the East Kunlun fault. After extending southward through Zhangla to Songpan, it continues to extend southward along the West Bank of Minjiang River to Jiaochang and Ma Laoding, and disappears in the area of animal husbandry shops north of Maoxian County. The Minjiang fault can be divided into three sections: north, middle and south, roughly bounded by the main temple of Sichuan and Jiaochang. In the southern section of Jiaochang, we can see the slope ridge landform formed by the thrust of the west wall of the fault on the Quaternary strata, and cut the Holocene slope diluvium staggeringly. In history, there were the earthquakes of M 7 in Diexi in 1713 and M 7.5 in Diexi in 1933. The active tectonic landform of Chuanzhusi-Bianchang section is slightly weaker, but new fault phenomena of Quaternary can still be seen, especially in the vicinity of Muerzhai and Songpannan. The new activity of Minjiang fault north of Chuanzhusi is more distinct. It is composed of three fault segments with different lengths and strikes, which are feather-like. The right-step feather-like zone between Gami Temple and Chuanpan is 3 km apart, which leads to the deformation of Minjiang River terrace. Near Hanpan-Shuijing, the Minjiang fault forms obvious fault scarps on Minjiang terrace and alluvial fan. The height of the fault scarp on the terrace surface ranges from 6 m to 10 m, and that on the alluvial fan is about 16 m. Through trench excavation, the steep fault ridge near Chuanpan reveals a thrust zone with a width of about 4 m formed by four to five reverse faults. The occurrence of the main fault is $N45^{\circ}E$, inclined to NW and dip angle is 40° . The gravels in the thrust zone are obviously arranged in a directional direction and have the general characteristics of overthrust faults. The top of the second terrace is a calcareous cemented gravel layer (the TL age of the top is $27000a \pm 2100a$), so the displacement marks are clear. The average vertical slip rate of the Minjiang fault since the late Pleistocene should be greater than and equal to 0.137 mm/a , because the displacement of the fault cannot be completely preserved until the river is cut down. The fault scarps on the Hanpancun alluvial fan have obvious retrogressive characteristics, with slopes ranging from 20° to 30° . Fine sand beds with rhythmic characteristics are deposited in the lower wall of the scarps (the TL age at the top is $30200a \pm 2300a$). Considering the general process of the steep ridge development of the reverse fault, the average vertical slip rate of the Minjiang fault since the Late Pleistocene should be less than 0.153 mm/a . Near Shuijing, the Minjiang fault passes through the surface of the Minjiang River terrace on the West Bank of the Minjiang River, forming two to three fault scarps which are nearly parallel and of varying height. The lowest fault scarp is 1 m-2 m high, the highest is 7 m-8 m, and the total height is about 10 m. In the gully of Shuijing, under the steep fault ridge, a reverse fault can be seen in the Quaternary gravel layer. The gravel layer on the upper wall of the fault bends slightly at the cross section, forming a towed anticline, and the gravel layer along the fault surface has obvious directional arrangement. In addition, several small gullies on the second-order surface are left-handedly dislocated by faults with a dislocation of about 10 m. The above phenomena indicate that the Minjiang fault shows the nature of reverse-strike-slip movement, and the horizontal dislocation is approximately equal to the vertical dislocation.

Based on the activity of the two boundary faults since the neotectonic period, it is likely that the Minshan fault block is formed by the differential movement of the Minjiang fault and Huya fault caused by the westward-eastward thrust. The starting time should be roughly from the end of Miocene to the beginning of Pliocene, which is related to the slip of the Chuanqing block towards the south-east-east direction. Geological evidence and modern

geodetic deformation data show that the slip process of the Sichuan-Qinghai block towards the southeast-east direction is still continuing, resulting in strong modern seismic activity in the Minshan fault block area.

Longmenshan Tectonic Belt

Maowen-Wenchuan Fault

In order to study the Maowen-Wenchuan fault, it is necessary to study the Maowen-Wenchuan fault in Maowen and Wenchuan counties. Firstly, the Maowen-Wenchuan fault in Maowen County is analyzed. The section of Maowen-Wenchuan fault in North brick factory of Maowen County is shown in Figure 6.

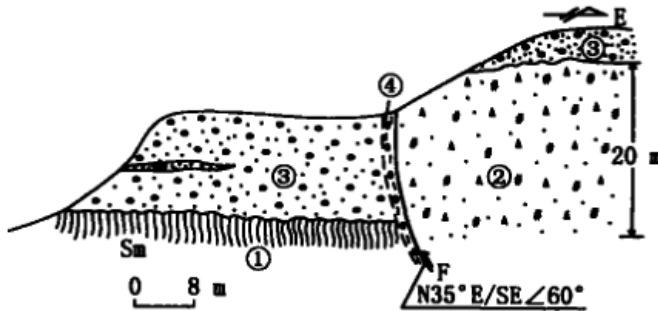


Figure 6. Maowen-Wenchuan fault profile

In Figure 6, ① shows phyllite and slate schist, ② shows bedrock fracture zone, ③ shows river facies gravel bed, and ④ shows directional arrangement of gravel. Through investigation and analysis, it is found that the right-handed dislocation of the first tributary of Minjiang River on the Maowen-Wenchuan fault reaches hundreds of meters. Although it is not yet possible to determine the starting time of faults after the formation of the river system and to exclude the influence of erosion, the synchronous dextral bending of the river system should be the geomorphological evidence of the dextral shear movement of the Maowen-Wenchuan fault and probably the cumulative displacement since the Quaternary. In the brick and tile factory north of Maowen County, we can see the fault river terrace of Maowen-Wenchuan fault. The bedrock fracture zone here is metamorphic phyllite, slate and schist of the Silurian Maoxian Group, with a visible width of 20 m-30 m (Sun, Zhao, & Wang, 2018). It directly thrusts over the sandy gravel layer of the third-grade River terrace. The occurrence of the fault is N35°E, with an inclination of SE and an inclination angle of 63°. A gravel orientation zone with a width of about 0.3 m to 0.5 m is formed along the section. In the middle of the terrace, the age of the sandy gravel layer determined by TL method is $23700a \pm 1900a$. Based on this, the average vertical slip rate of the fault since late Pleistocene is estimated to be about 0184mm/a. Secondly, the Maowen-Wenchuan fault in Wenchuan county area is studied. The paleoearthquake sand veins in Wenchuan county area are shown in figure 7.

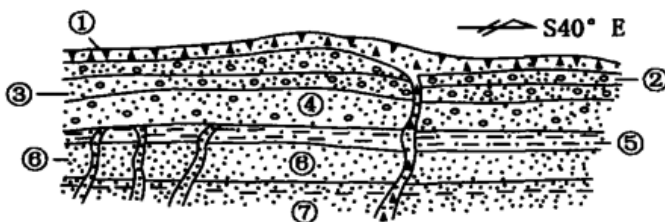


Figure 7. Paleo-seismic sand veins of sand gravel layer in Jiangwei City, Wenchuan River terraces

In Figure 7, ① shows the gray-yellow slope alluvial gravel layer, ② represents the brown-gray sand with sub-prismatic breccia, ③ represents the coarse sand, ④ represents the brown-gray gravel, ⑤ represents the yellowish-

brown fine sand, ⑥ represents the yellowish-yellow fine sand, and ⑦ represents the green-gray fine-silt. In Jiangweicheng on the South Bank of Minjiang River in Wenchuan County, there are compressive-torsional faults in Alluvial-diluvial strata with 120 m high river bed. The faults strike N30°E, with an inclination of SE and an inclination angle of 70° and form "entry" structure with the main faults, indicating the right-lateral dislocation of the faults. In addition, there is a group of sand veins in Alluvial-diluvial gravel strata corresponding to the elevation of river terraces in Jiangweicheng. The width of sand veins is generally 0.5 cm-1 cm, and the maximum width is 3 cm-5 cm, which may be two paleoearthquake events.

Beichuan-Yingxiu Fault

Beichuan-Yingxiu fault is mainly studied in Yingxiu area and Dongxujiagou of Baishuihe River. Firstly, Beichuan-Yingxiu fault near Yingxiu is studied. The section of North East wall of Beichuan-Yingxiu fault exploration trough in this area is shown in Fig. 8.

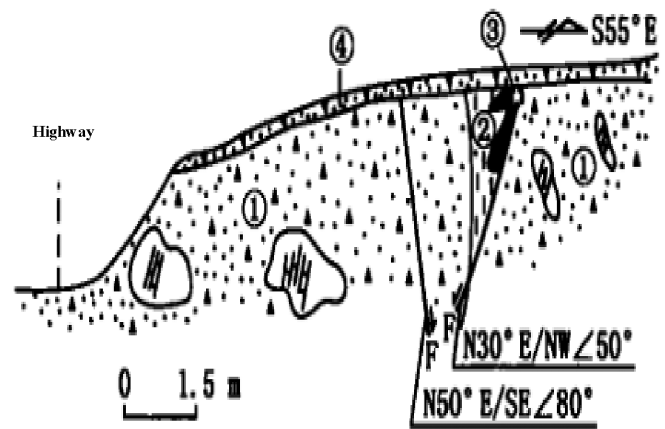


Figure 8. Profile of the north east wall of the Beichuan-Yingxiu fault exploration trough in Yingxiu area

In Figure 8, ① is brown red clay with limestone fragments, ② is yellowish clay, ③ is black clay with peat, and ④ is modern humus layer. It can be seen from the graph that the Beichuan-Yingxiu fault near Yingxiu extends in the direction of N60-70°E. Some scholars have studied the phenomenon of Pengguan complex thrusting over the Quaternary fluvial sandy gravel bed in the north-west wall of the fault. In Yingxiu substation, a NE trench with a length of about 100 m, a width of about 20 m and a depth of about 5 m is formed on the terrace surface of the Minjiang River, and a steep ridge with a height of about 40 m is formed on the terrace surface, which is suspected to be caused by the vertical fault of the fault. For this reason, TL samples are collected on both sides of suspected faults. The age values measured are $76360a \pm 6490a$ and $73000a \pm 6200a$, which are close to each other. It is confirmed that the same terrain is the fault scarp caused by differential movement of faults. This section can be interpreted by the model of structural deformation of thrust faults: the upward thrust of the NW wall of the Beichuan-Yingxiu fault forms a fault ridge on the fourth-order surface, while the bending fault is formed on the upper wall of the thrust faults due to local tension, and the trench in the form of graben is formed by the downward action of the bending fault. The average vertical slip rate of Beichuan-Yingxiu fault is estimated to be about 0154mm/a according to the height of the fault scarp and the age of terrace surface.

Secondly, the Beichuan-Yingxiu fault in Xujiagou area in the east of Baishui River is studied. The Beichuan-Yingxiu fault presents better linear image characteristics in aerial photographs. The slope of slope-cut mountain forms a typical landform of slope trough. The northwest plate of the fault declines relatively to form a fault-plug pond, which strictly restricts several smaller Holocene pluvial fans. On the north-west side of the fault, there are some abandoned gullies in the south-east wall. It is estimated that the average

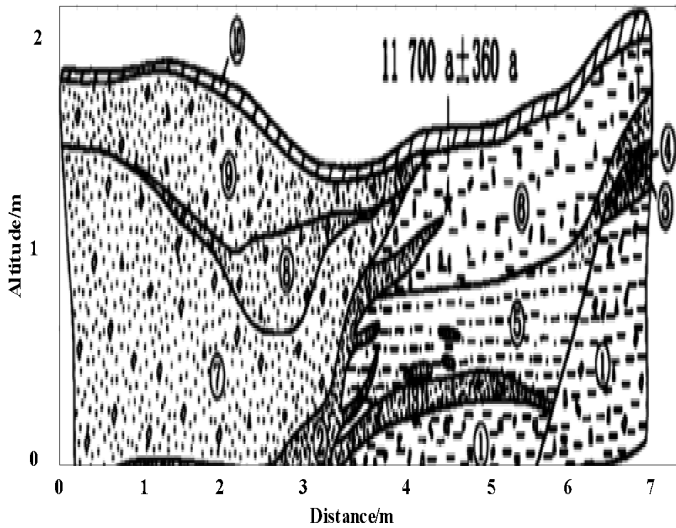


Figure 9. Cross-section of the north-east wall of the north-east wall of the north-to-the-show break in the vicinity of the Jiajiagou

horizontal slip rate of the fault since late Pleistocene should be between 0182 mm/a and 113 mm/a, and the average value is about 1.1 mm/a. In addition, near Fengyanzi, a small gully in Beichuan-Yingxiu fault which will develop on the third terrace surface has a dextral dislocation of 10 m, but the starting time of the dislocation is unknown. A groove about 7m in length is laid in a broken plug pond. The structure of the groove is shown in Figure 9.

In Figure 9, ① is brown-black gravel with clay and charcoal wood, ② is grey-black clayey silt, ③ is grey-white coarse sand with gravel, ④ is grey-black sand with gravel and charcoal, ⑤ is grey-white clay, ⑥ is brown-yellow sandy clay, ⑦ is brown sand with gravel, ⑧ is blue-gray coarse sand with gravel, and ⑨ is yellow-black gravel with clay. Two paleo-seismic events can be identified from the profile of the trough. Seismic fault cutting events occurs in event 1 and seismic fault cutting events occurring in event 2 cut layer ①, ③ and ④, resulting in vertical faults of about 800mm, which are sealed by layer ⑤. Sedimentary characteristics of layer 5 are obviously controlled by the fault scarp shape at that time, and under the fault. The dish is gray-white clay and the upper dish is gravel with sandy soil. The time of the earthquake is after $21910a \pm 290a$. Event 2 results in the liquefaction of grey-black clayey silt of layer ②, which penetrates upward into the overlying stratum (Pan, Yang, & Zhu, 2018). The upper stratum of vein sand penetrated upward is the middle part of the brown-yellow sandy clay of layer ⑥. It is estimated that the layer ⑥ has been deposited and is in a saturated state at that time, so when the earthquake occurs, the interval is after $11770a \pm 360a$.

Discussion

Through the analysis of Cenozoic structures in the eastern margin of the Qinghai-Tibet Plateau, it is found that Xigeda lacustrine facies deposits in the eastern margin of the Qinghai-Tibet Plateau are distributed in the Dadu River, Anning River and Jinsha River basins. Detailed magnetostratigraphic studies show that the main body of the strata is Gaussian deposits, which is a good record carrier of Paleoenvironmental change information in the P Sedimentation. Xigeda Formation in Luding is the earliest, about 4.2 Ma to present, and that of Mianning and Honggexigda Formations is about 0.6 Ma later. The sedimentary records of Xigeda Formation have many regular change periods. The sedimentary records of Mianning section show that the sedimentary environment of 3.2 MaBP has changed greatly. The sedimentary records of Luding section show that the strong uplift of Qinghai-Tibet Plateau has begun at 2.8 MaBP. The Xigeda ancient lake is a water-crossing lake, and the Xigeda ancient lake completely disappears at 2.6 MaBP. The Pan-lake period on the eastern margin of the Qinghai-Tibet Plateau is ended at the end of Pliocene. In the early Quaternary, the river-lake facies strata only appears in Daqingliangzi, Xichang. Glacier and river deposits are the main deposits in the region, and the paleoclimatic environment changes greatly. At this time,

typical wind-dust deposits appears on the Loess Plateau, which is closely related to the uplift of the Qinghai-Tibet Plateau. In the eastern margin of the Qinghai-Tibet Plateau, there are many glacial periods in the Late Cenozoic. In addition to the three glacial periods since the penultimate glacial period, three sets of moraines are developed earlier. Haiziping moraine layer in Luding represents the 4.3 Ma old glacial age in the eastern margin of the Qinghai-Tibet Plateau. During the Quaternary period, there are five glacial periods, forming at 2.2 MaBP, 1.1 MaBP, 0.6-0.7 MaBP, 0.2 MaBP, 0.01 MaBP-0.07 MaBP, respectively. The paleoglacial sequence in the eastern part of the Qinghai-Tibet Plateau is preliminarily established, which deepens the understanding of the Late Cenozoic glaciers in the "Third Pole of the Earth".

With the continuous change of time, the structure of the eastern margin of the Qinghai-Tibet Plateau is analyzed. Current horizontal movement reflected by regional GPS observations has the difference of spatial distribution and time-varying stages. The difference of horizontal movement intensity and mode in different tectonic zones is controlled by NE-oriented compression, E-oriented extrusion and rotation around the eastern tectonic junction of the Qinghai-Tibet Plateau, and the periodicity of movement state changes with time (especially in the eastern tectonic junction). The strain energy accumulated in the Wenchuan earthquake-generating section of Longmenshan tectonic belt under long-term compression and locking is in a state of relaxation and adjustment after the concentrated release of large earthquake of M 8.0, but the tectonic location associated with it and the western Qin Dynasty in the periphery are in a state of relaxation and adjustment. The strain accumulation in the tectonic zones such as the eastern boundary of the western Qinling and Sichuan-Yunnan rhombic blocks may continue.

Based on the above data, several main faults in Longmenshan tectonic belt have shown thrust movement from NW to SE since late Quaternary, and have significant dextral strike-slip components. The average vertical slip rate of a single fault is about 1 mm/a, and the horizontal dislocation is approximately equal to the vertical dislocation, which is consistent with the conclusion that the average crustal shortening rate in Longmenshan area measured by GPS is less than 3 mm/a. According to the available paleoseismic data, the Beichuan-Yingxiu fault and the Maowen-Wenchuan fault both have a history of strong earthquake activity before history. Although the current data are not enough to directly determine the magnitude of paleoearthquakes, the magnitudes of earthquakes causing surface ruptures and dislocations in Western China are generally above 6 or 7, it can be roughly determined that these two main faults have the ability to produce earthquakes of about 7 magnitudes. According to the research results of Beichuan-Yingxiu fault, it can be judged that the last strong earthquake occurred not long after $3830a \pm 200a$, based on the historical seismic records of Chengdu area for more than two thousand years. The recurrence interval of strong earthquakes on the single fault of these two main faults should be at least 2000-3000a.

Conclusions

The eastern margin of the Qinghai-Tibet Plateau is one of the areas with the strongest neotectonic movement, strong earthquake activity and internal and external dynamic coupling. This is not only an important window to deeply understand the uplift process of the Qinghai-Tibet Plateau and its environmental disaster effects and to understand the crustal deformation process and its dynamic mechanism of the East Asian continent, but also a bridgehead for the development of the western part of China. It is the most densely populated area in Western China, among which many major national transportation and hydropower projects are being implemented and will be implemented. Therefore, a comprehensive understanding of the basic characteristics and evolution of geological structures in the eastern margin of the Qinghai-Tibet Plateau, a detailed identification of the distribution of major active faults and their geometric and kinematic characteristics, and a thorough exploration of the glacier geological characteristics and three-dimensional crustal movement characteristics in the area are all very significant geological foundations of theoretical significance and application value. Through theoretical analysis and practical investigation, it is found that the eastern margin of the Qinghai-Tibet Plateau has been characterized by typical tectonic deformation of the intracontinental regenerative orogenic belt since Quaternary. Several pre-existing main faults are reversed-strike-slip faults, indicating both crustal

shortening and horizontal slip. From this point of view, the eastward escape of crustal material in the Qinghai-Tibet Plateau does exist. However, from the slip rate values of several main faults since late Quaternary, it can be judged that the crustal material escape rate is much less than the estimated 20 mm/a, which is roughly consistent with the results of less than 3 mm/a measured by GPS nowadays.

Acknowledgement

The study was supported by “National Natural Science Foundation of China (No.51508484)”

Reference

- Bu, H. Y., Wang, X. J., Zhou, X. H., Qi, W., Liu, K., Ge, W. J., ... Zhang, S. T. (2016). The ecological and evolutionary significance of seed shape and volume for the germination of 383 species on the eastern Qinghai-Tibet plateau. *Folia Geobotanica*, 51(4), 333-341.
- Chen, J., Zhao, L., Sheng, Y., Li, J., Wu, X., Du, E., ... Pang, Q. (2016). Some Characteristics of Permafrost and Its Distribution in the Gaize Area on the Qinghai—Tibet Plateau, China. *Arctic Antarctic & Alpine Research*, 48(2), 395-409.
- Feng, D. X., Gao, X. Q., Yang, L. W., Hui, X. Y., & Zhou, Y. (2017). A spatial-temporal distribution characteristics of the atmospheric methane in troposphere on Qinghai-Tibetan plateau using ARIS data. *China Environmental Science*, 37(8), 2822-2830.
- He, H. L., Yang, X. C., Li, D. D., Yin, C. Y., Li, Y. X., Zhou, G. Y., ... Liu, Q. (2017). Stoichiometric characteristics of carbon, nitrogen and phosphorus of *Sibiraea angustata* shrub on the eastern Qinghai-Xizang Plateau. *Chinese Journal of Plant Ecology*, 41(1), 93-98.
- Hu, G., Lin, Z., Wu, X., Li, R., Wu, T., Xie, C., ... Cheng, G. (2016). An analytical model for estimating soil temperature profiles on the Qinghai-Tibet Plateau of China. *Journal of Arid Land*, 8(2), 232-240.
- Jiang, L., Ruan, Q., & Chen, W. (2016). The complete mitochondrial genome sequence of the Xizang Plateau frog, *Nanorana parkeri* (Anura: Dicroglossidae). *Mitochondrial Dna*, 27(5), 1-2.
- Jie, L., Ya, H. L., De, Z. L., & Gao, L. (2017). Evolution and maintenance mechanisms of plant diversity in the Qinghai-Tibet Plateau and adjacent regions: retrospect and prospect. *Biodiversity Science*, 25(2), 41-45.
- Li, J. L., Zheng, B. L., & Peng, Y. Z. (2018). Study on diffusion stress of cylindrical gradient electrode based on Gibbs free energy variation. *Chinese Journal of Power Sources*, 42(9), 38-41+155.
- Liu, C., Cai, X., & Chen, Q. (2018). Research on chain STATCOM with Energy Storage function. *Journal of Power Supply*, 16 (4):21-27.
- Pan, W. J., Yang, L., & Zhu, X. P. (2018). Modeling of Colored Petri Nets in the Operation process of busy Airport apron. *Computer simulation*, 35(1), 52-56.
- Sun, J. J., Zhao, Y., & Wang, S. G. (2018). Improvement of SIFT feature matching algorithm based on Image gradient Information Enhancement. *Journal of Jilin University (Science Edition)*, 56(1), 82-88.
- Wang, L., Tang, J., & Wang, X. D. (2017). Geological characteristics of lead-zinc ore deposits in Qinghai-Tibet Plateau. *Science & Technology Review*, 35(12), 83-88.
- Wang, Z. (2017). Geological features, the formation and the evolution of the Qinghai-Tibetan Plateau. *Science & Technology Review*, 35(06), 51-58.
- Wan, Q., & Du, X. X. (2018). Research on the Application of Industrial Development Network Model based on Evolutionary Network in Science and Technology Management. *Automation & Instrumentation*, 1(6)25-29
- Wei, Y., Guo, X., Yao, T. Zhu, M., & Wang, Y. (2016). Recent accelerating mass loss of southeast Tibetan glaciers and the relationship with changes in macroscale atmospheric circulations. *Climate Dynamics*, 47(3-4), 805-815.
- Xiao, Q., Tan, J., Hu, H., Zhou, S. D., & He, X. (2017) . *Semenoviagyirongensis*(Apiaceae), a new species from Xizang, China. *Phytokeys*, 82(82), 57-72.
- Yang, W., Miao, L. L., Dan, Y. U., Liu, C. H., & Wang, Z. (2017). Effects of environmental factors on gross caloric values of three life-forms aquatic plants on the Qinghai-Xizang Plateau, China. *Chinese Journal of Plant Ecology*, 41(2), 209-218.
- Yi, W., & Wang, C. (2016). Features of clouds and convection during the pre- and post-onset periods of the Asian summer monsoon. *Theoretical & Applied Climatology*, 123(3-4), 551-564.
- Zhang, B. B., Liu, F., Ding, J. Z., Fang, K., Yang, G. B., Li, L., ... Yang, Y. (2016). Soil inorganic carbon stock in alpine grasslands on the Qinghai-Xizang Plateau: An updated evaluation using deep cores. *Chinese Journal of Plant Ecology*, 40(2), 93-101.
- Zhang, Z. Y., Liu, F., & Huang, L. Y. (2017). Influence of cross section shape of electromagnetic track launcher on emission performance. *Journal of China Academy of Electronics and Information Technology*, 12(5), 513-517.

